Pergamon

Planet. Space Sci., Vol. 45, No. 1, pp. 39–48, 1997

0032–0633/97 $17.00+0.00

PII: S0032–0633(96)00093–1

Planetary gamma-ray spectroscopy of the surface of Mercury

J. Brückner and J. Masarik

Max-Planck-Institut f. Chemie, Abt. Kosmochemie, Postfach 3060, D-55020 Mainz, Germany

Received 3 October 1995; revised 29 April 1996: accepted 29 April 1996

Abstract. To approach basic scientific questions on the origin and evolution of Mercury one needs data on its chemical composition. Gamma-rays emitted from the surface can be measured by a gamma-ray spectrometer on board an orbiting spacecraft. The gamma-ray flux emitted by the surface of Mercury is simulated by Monte-Carlo codes that calculate the interaction of cosmic-ray particles with the surface and the subsequent gamma-ray production. Different surface compositions are assumed for these calculations. The calculated gamma-ray data allow a clear distinction of the different surface compositions. Also, the ability to detect water buried in the polar zones is taken into consideration: small amounts of water will be seen in the gamma-ray data. Applying the Monte-Carlo technique in an iterative process, measured gamma-ray data can be converted into elemental concentrations of many elements present in the surface. A detector with excellent energy resolution is required to fully exploit the complex gamma-ray spectra. A cooled germanium detector would be the best choice for this task, provided constraints on mass and power can be solved in the near future.

Introduction

The planet Mercury is an end member for the terrestrial planets in respect to its mass, density, and heliocentric distance. Mercury puts constraints on models for the origin and evolution of terrestrial planets. Therefore, exploring Mercury by space missions will provide essential data for the formation of all terrestrial planets. Planetary gamma-ray spectroscopy can provide a significant contribution to the exploration of Mercury.

Since Mercury has no atmosphere and only a very weak magnetic field the energetic galactic cosmic rays are permanently bombarding its surface. The resulting interactions of the particles with matter are the main sources of gamma-rays. Since the production process and transport of secondary particles is very complex, the major portion of the gamma-rays belongs to a continuum, a rather featureless distribution of gamma-ray energies spread over a range from about several 10 MeV down to tens of keV. Discrete-energy gamma-rays are produced by typical reactions inside the surface, such as (n,nγ) inelastic reactions and (n,γ) capture reactions of fast and thermal secondary neutrons, respectively. These gamma-rays that carry information about the nucleus which emitted them are diagnostic for the composition of the surface material and can be used as an analytical tool. Their specific very sharp energies are used for the identification of the emitting nuclei, i.e. the elements present in the surface, while their intensities reflect the concentration of the elements. So, qualitative and quantitative remote analysis of the planetary surface is possible and can be done successfully by using a high-resolution gamma-ray detector, such as a high-purity germanium detector (Brückner *et al.*, 1987). An orbiting spacecraft could carry a gamma-ray spectrometer on board, and gamma-rays emitted by the Mercurian surface could be measured over a long period of time. From the accumulated gamma-ray spectra, the elemental composition of the surface can be derived, which will put constraints on models of the formation and evolution of Mercury (Brückner *et al.*, 1994).

State of the art

Very early work on planetary gamma-rays dates back to Arnold (1958) and Metzger *et al.* (1962) in planning for the lunar Ranger missions and to Vinogradov *et al.* (1967) for the Luna 10 results. The Ranger gamma-ray spectrometer (GRS) only measured interplanetary gamma-ray fluxes (Arnold *et al.*, 1962; Metzger *et al.*, 1964). The Luna 10 spectra were of low quality, but have been used by Surkov (1984) to estimate levels of radioactivity on lunar regions.

The APOLLO gamma-ray spectrometers (AGRS) on

Correspondence: J. Brückner

the Apollo 15 and 16 missions in 1971 and 1972, respectively, produced the first good gamma-ray data from another planet. The AGRS consisted of a NaI(Tl) scintillation detector surrounded by a plastic scintillator shield to reject charged particles (Harrington *et al.*, 1974). The first results of the AGRS were maps of lunar radioactivity (Metzger *et al.*, 1972). As the NaI detector has poor energy resolution, considerable efforts were involved in getting elemental results from the AGRS data. Different methods were developed to improve the elemental analysis or the spatial resolution (see Bielefeld *et al.* (1976), Metzger *et al.* (1977) and Reedy (1979) and references therein). Further studies using AGRS data gave results that were consistent with lunar sample results (Spudis and Hawke, 1981; Davis and Spudis, 1985, 1987).

In 1989, one of the two Phobos spacecrafts reached an orbit around Mars and, before "Phobos 2" also was lost, a few gamma-ray spectra of the Martian surface could be accumulated by a large CsI scintillation detector. These spectra, which had low counting statistics, were analysed by Surkov *et al.* (1989). Trombka *et al.* (1992) re-evaluated the Phobos spectra independently and obtained similar compositional results.

Some of the scientific objectives of the NASA Mars Observer mission were (1) the determination of the elemental composition of the Martian surface including poles, (2) the geochemical characterization of the different regions, and (3) the search for water and other volatiles. A germanium GRS was considered the appropriate instrument (Arnold *et al.*, 1989) and was designed to measure gamma-rays and neutrons that emerge from the planetary surface (Boynton *et al.*, 1992). The Mars Observer Gamma-Ray Spectrometer (MO GRS) turned out to be a very successful instrument during the cruise phase. It operated many weeks successfully and measured gamma-rays emitted by the spacecraft and the instrument itself (Englert *et al.*, 1994), however, just 3 days before Mars orbit insertion (August, 1993), communication with Mars Observer was lost. The MO GRS demonstrated the feasibility of flying a high-resolution, solid-state HPGe detector in space with successfully passive cooling. Based on this experience, germanium GRS are considered to be mature. NASA is planning to have a GRS on board of one of the follow-on missions to Mars.

An attractive design to compensate to some extent the poor energy resolution of a scintillation detector is (1) to surround it with a large BGO scintillation shield and (2) the simultaneous usage of large-area X-ray detectors. This concept will be carried out by the X-ray/gamma-ray spectrometer (XGRS) on board the orbiter of the NASA Near Earth Asteroid Rendezvous (NEAR) mission (Trombka *et al.*, 1995). Launch of the spacecraft will be in February 1996 and rendezvous with the asteroid Eros in 1999.

On Mars-96, a Russian Mars mission to be launched in November 1996, there will be several gamma-ray detectors on board for orbital measurements: the PHOTON GRS consisting of two CsI scintillators, one surrounded by a bismuth germanate (BGO) collimator and one bare; and the "High Precision Gamma-Ray Spectrometer" (PGS) containing two large germanium detectors with a passive cooling device (Mitrofanov *et al.*, 1995).

An advanced BGO GRS will be flown during the NASA discovery mission "Lunar Prospector" (Asker, 1995), while a HPGe GRS was considered for MORO, a potential European Space Agency (ESA) mission to the Moon (Chicarro *et al.*, 1994).

Recently, the most lightweight HPGe GRS was preselected to be on board of Champollion, a device to be landed on the surface of a comet during the ESA Rosetta mission sometime after the year 2010 (d'Uston *et al.*, 1996).

Even further ahead in the future are plans by ESA to explore the planet Mercury (Grard *et al.*, 1994). Such a mission is considered as a possible cornerstone of the ESA "Horizon 2000 plus" plan. On the primary model payload a gamma-ray spectrometer is listed. Therefore, we report on extended studies of gamma-ray spectroscopy of Mercury.

Evolution of Mercury

Little is known about the planet Mercury, since terrestrial observations are very difficult because of the close proximity to the Sun and, second, so far only one spacecraft, the American Mariner 10, visited Mercury in three flybys. From this visit the high density (5.4 g cm^{-3}) of Mercury was confirmed (Anderson *et al.*, 1987), which emphasized the puzzle that Mercury is too heavy compared to the volume of other terrestrial planets. There are a variety of models to explain the high density of Mercury in respect to its possible origin and evolution. We will only briefly mention a few models, just to outline what to expect when making gamma-ray measurements of the Mercurian surface. To achieve a discrimination of these models the elemental composition of the Mercurian surface has to be determined, since its composition is the result of ancient evolution processes. A gamma-ray spectrometer would be an appropriate tool to fulfil this task.

In general, one can assume that Mercury contains a large core (about 70% metallic phase) and a relatively small mantle (30% silicate phase); this would be about twice the Fe/Si bulk ratio of any known terrestrial planet. One scenario is that due to unspecified processes in the early solar nebula the iron/silicon ratio in the feeding zones of the proto Mercury was changed compared to accretion zones of the other terrestrial planets. However, about a fivefold increase of the Fe/Si ratio is required to account for an iron core of the size needed. One could speculate that in the proximity of the Sun the conditions were highly reducing so that other elements like silicon would become metallic and hence contributing to the core phase. As a consequence the Mercury mantle and crust should contain only very little FeO (Wänke and Dreibus, 1986a). This leads to an overall very low (maybe almost zero) Fe content of the surface, easily to be determined by a gamma-ray spectrometer.

A second class of models uses vaporization by applying the different volatilities of iron and silicates to fractionate the two phases (Cameron, 1985). Volatility effects would lead to large chemical fractionations, and the silicate phase would undergo large compositional changes. The silicate phase would be depleted in alkalis, FeO and SiO_2 and enriched in CaO, MgO, Al_2O_3 and TiO_3 relative to

chondritic material (Cameron *et al.*, 1988). This could be detected from orbit.

A third class of models assumes that the accretion of Mercury was similar to other terrestrial planets. Later in its history, Mercury suffered from one or several giant impacts leading to the loss of a substantial portion of the mantle. At that time, the new surface resulted from the reaccumulation of larger collision fragments, which may have been "contaminated" by residuals from impacting projectiles (see Wetherill (1988) and Cameron *et al.* (1988) and references therein). Also, this scenario would be reflected in the composition of its surface.

In addition, the geochemical behaviour of the radionuclides potassium and uranium (and thorium) would reveal if the so-called "K/U ratio" fits into the range of values known for terrestrial bodies. During condensation of the solar nebula, the volatile character of K and the refractory nature of Th and U could have followed the general temperature profile of the primitive solar nebula. Decreasing temperatures as a function of growing distance from the Sun would have increased the K/U (and K/Th) ratio with solar distance (Table 1). The hitherto unknown K/U ratio of Mercury could shed light on its former position in the solar nebula during accretion (indicating possible large orbital changes). As outlined in some vaporization models, a huge loss of K occurs during the vaporization process, while also some U is lost compared to Th, which essentially remains undepleted (Cameron *et al.*, 1988). Only gamma-ray spectroscopy can detect the radionuclides K and Th and to a lesser extent U. Provided their concentrations are high enough, their abundances can be determined or, at least, upper concentration limits can be derived.

Model for simulation of gamma-ray production

Our model for the simulation of the interaction of primary and secondary galactic-cosmic-ray particles with matter, including reactions in which gamma-rays are produced, is based on the LAHET Code System (LCS) (Prael and Lichtenstein, 1989), which is a system of general-purpose Monte-Carlo computer codes, that treats the relevant physical processes of particle production and transport. In these codes, incident primary particles are transported through matter considering atomic (mainly ionization energy losses) and nuclear interactions. In these nuclear interactions, new (secondary) particles are produced and subsequently transported with their interactions modelled. The LAHET (Los Alamos High Energy Transport) codes transports and models the interactions of all charged particles (protons, alpha particles, pions, and muons) and neutrons with energies greater than 15 MeV. Neutrons produced with energies less than 15 MeV by the interactions modelled by LAHET are transported and have their interactions calculated with the MCNP (Monte-Carlo N-particle) code (Briesmeister, 1993), which was designed for such neutron calculations. The LAHET code models nuclear interactions using parameters designed for all nuclei (global parameters) while MCNP uses a library of evaluated cross-sections for each neutron reaction. These codes have been frequently tested for a large variety of applications. More details on LCS and its application to cosmic-ray interactions in matter are given in Masarik and Reedy (1994a, 1996).

While LCS can calculate gamma-ray line fluxes as one of its outputs, we used this option only for rates of neutron-capture reactions, where the MCNP code is coupled to very massive libraries that contain state-of-the-art neutron capture cross-sections, and for estimations of the gamma-ray continuum. In all other cases we used LCS only to calculate the fluxes of particles that lead to gamma-ray production. We are convinced that LCS and similar codes are better at calculating particle fluxes than direct gamma-ray production, because the measured cross-sections used in particle production and transport are much more accurate than those used for the production of gamma-rays in inelastic neutron reactions.

Assuming isotropic irradiation of a sphere with radius R by GCR particles, the production rate of nonelastic-scattering and capture gamma-ray j at a depth D is

$$P_j(R, D) = \sum_i N_i \sum_k \int_0^\infty \sigma_{jik}(E_k) \cdot J_k(E_k, R, D)\, \mathrm{d}E_k \qquad (1)$$

where N_i is the number of atoms for target element i per kg material in the sample, σ_{jik} the cross-section for the production of gamma-ray j from target element i by particles of type k with energy E_k, and $J_k(E_k, R, D)$ the total (primary plus secondary) flux of particles of type k with energy E_k at location D inside their radiated body. This expression is very similar to the one in Masarik and Reedy (1994a,b, 1996) that has been successfully used for the calculation of cosmogenic nuclide production in meteorites and gamma-rays in Mars. As stated earlier, the particle fluxes $J_k(E_k, R, D)$ are calculated using LCS, and the cross-sections σ_{jik} were ones evaluated from many measurements and used in earlier gamma-ray-flux calculations by Reedy *et al.* (1973) and Reedy (1978). There have been some cross-sections measured for the production of nonelastic-scattering gamma-rays since then, but few reactions would have cross-sections much different from those used here.

A strong source of gamma-rays, which contributes to the background in the gamma-ray spectrum, are the neutral π^0 mesons generated in large numbers in high energy interactions of primary and secondary particles. Their contribution was calculated by the PHT code (Prael and Lichtenstein, 1989). In PHT, neutral π^0 mesons decay into two gamma-rays at the site where they are created, which is justified by the very short half-life of π^0 mesons (8.7×10^{-17} s). These gamma-rays are transported and usually produce a cascade of lower-energy gamma-rays (Armstrong, 1972; Dagge *et al.*, 1991).

Table 1. K/U ratio for CI meteorite and terrestrial bodies

	CI meteorites[a]	Mars as SPB[b]	Earth[c]	Venus[d]	Mercury
K/U	63,000	19,688	11,000	8000?	??

[a]Wänke and Dreibus (1986b).
[b]Burghele *et al.* (1983).
[c]Wänke (1987).
[d]Surkov *et al.* (1975).

In going from the source (surface) to the detector, a gamma-ray can vanish entirely (e.g. photo effect) or its multiple interactions within the planetary body (e.g. Compton scattering) can produce a continuous spectrum in the energy range of interest. The total gamma-ray spectrum is thus the sum of the gamma-ray line spectrum, the photons from π^0-decay, and this continuous spectrum. As in almost all applications of gamma-ray spectroscopy, only gamma-rays that arrive at the detector without changing energy are used for mapping elements, so we concentrated our attention on them. The gamma-ray continuum contains some elemental information (Thakur and Arnold, 1993) but was not modelled in detail here.

Gamma-rays from natural radioactivity

The gamma-rays made by the decay of the naturally radioactive elements of potassium (^{40}K), thorium (^{232}Th), uranium (mainly ^{238}U), and the daughter isotopes of U and Th are important in planetary studies. Details on the production of these gamma-rays and their transport to the surface assuming a constant concentration with depth are described in Reedy *et al.* (1973) and Reedy (1978). The decay parameters used are those in Reedy (1978). The mass attenuation coefficients used for the transport of these gamma-rays are described below.

Galactic cosmic-rays

The simulation of particle production and transport processes begins with a choice of the primary particle type and its energy. Mercury's surface was irradiated by a homogeneous, isotropic particle flux. Reedy (1978) gave a list of gamma-rays resulting from nuclear reactions induced by solar-cosmic-ray (SCR) particles striking the Moon. Such sources of gamma-rays are more important for Mercury, because the long-term average flux of SCR particles in the solar system varies roughly inversely with the square to cube of the distance from the Sun (Shea *et al.*, 1988). Therefore, their fluxes at Mercury are a few times higher than those at the Moon. Since solar protons are the least important of all the gamma-ray sources, the inability to predict solar-proton-induced gamma-ray fluxes for Mercury will not be a serious problem. The combination of measured fluxes of more gamma-ray lines from the same target element could be used to convert the obtained results to absolute abundances.

Galactic cosmic-rays consist of 87% protons, 12% alpha particles, and 1% heavier nuclei with atomic numbers from 3 to ~90 (Simpson, 1983). If energies are expressed as per-nucleon values, the spectral distribution of the heavier particles is quite similar to that for protons. The GCR particles are influenced by many interactions that lead to spatial and time variability of their fluxes. Among them, probably the dominant is solar modulation, which is taken into account in the expression for the differential GCR proton flux (Castagnoli and Lal, 1980), with modulation parameter Φ. We used this expression elsewhere (Masarik and Reedy, 1994a, 1996; Michlovich *et al.*, 1994) for calculations involving GCR particles. In our calculations we used only one value of the modulation parameter, $\Phi = 550$ MeV, which is very close to the one used for describing the GCR flux averaged over a solar cycle (Reedy, 1987). The percentage of alpha particles in the primary GCR spectrum is fairly high (the ratio of alpha-particles to protons is ~0.14, and therefore, they have to be considered in every precise Monte-Carlo simulation. The contribution of alpha particles is included only in our final results by normalizing the proton calculations by a scaling factor, which was found on the basis of previous calculations to be 1.4. The results presented in this paper are based on calculations, in which we simulated the irradiation using 100,000 primary GCR protons with energies and spectral distribution given by Castagnoli and Lal (1980). Because of the lack of suitable cross-sections for the production of gamma-rays in proton-induced reactions, the nonelastic-scattering gamma-ray fluxes presented here do not include production by protons. On the basis of analysis carried out in Masarik and Reedy (1996), we estimate their contribution to the total gamma-ray fluxes on the level of 8–10%.

Gamma-ray production and transport

The source term, that is the rate at which gamma-rays are produced, is, for gamma-rays emerging from neutron capture and neutron nonelastic-scattering reactions, calculated according to equation (1). As the flux of particles that induce nuclear reactions, in which gamma-rays are produced, is depth dependent, the source term is usually also depth dependent. A source term that is uniform with depth is the only one used for natural radioactive isotopes, as described above. Statistical errors of particle fluxes using this geometrical model and running 100,000 primary particles were at the level of 3–4% for neutron fluxes at all relevant depths as well as for proton fluxes near the surface, and 5–6% for proton fluxes at depths of 100 g cm^{-2}. The systematic uncertainties in our calculated fluxes are not known exactly, but they are probably of the order of 10%.

In our calculations we are not concerned with scattered photons, but only with the photons that undergo no interactions before they reach the detector. Their flux, which is defined as the intensity of photons reaching a unit-area isotropic detector above the planetary surface, was calculated. Once the source term is known, the transport of the gamma-rays from their point of creation to the detector must be considered. In most cases, the gamma-ray detector will be above the planet's surface, such as on an orbiting satellite. The flux at a spacecraft above Mercury varies with the spacecraft altitude. In the calculation of fluxes at the detector, the geometry and effects related to the attenuation in passing through the Mercury surface had to be included.

An important parameter in calculating the gamma-rays that escape from a planet with their original energy is the exponential mass attenuation coefficient in each medium through which the gamma-rays pass. The fraction of gamma-rays that pass through a thickness d of matter (in g cm^{-2}) is $\exp(-\mu d)$ (i.e. over a path length of $1/\mu$, the intensity of the gamma-ray flux decreases by a factor $1/e$). Gamma-ray attenuation coefficients are functions of

gamma-ray energy and of the medium's composition, and therefore, they were calculated for each gamma-ray line and each composition used in calculations.

For planetary gamma-rays, coherent scattering (photon changes direction but not its energy) is ignored. Elemental gamma-ray attenuation coefficients were calculated from the total and coherent cross-sections. Tables for cross-sections for the total scattering (which included coherent scattering) and for coherent scattering only were used to get a total-less-coherent cross-section. The cross-sections were from Plechaty *et al.* (1981), which are in good agreement with other attenuation-coefficient compilations. For a mixture with weight fraction w_i of the ith element (with $\Sigma_i w_i$ normalized to unity), the attenuation coefficient is $\Sigma_i w_i \mu_i$.

The calculation of the gamma-ray flux reaching the planetary surface and a detector on the surface was done similarly to that by Reedy *et al.* (1973) and Masarik and Reedy (1996). If the detector is above the planetary surface the gamma-ray flux at altitude H can be calculated from the gamma-ray source term as

$$F = \int_0^{2\pi} \mathrm{d}\varphi \int_0^{l_{\max}} \int_0^{\beta_{\max}} P_j(R, D) \cdot \sin\beta \cdot \mathrm{e}^{-\mu_s \cdot l(\beta)} \cdot \mathrm{d}l \cdot \mathrm{d}\beta \quad (2)$$

where $\beta_{\max}$ is the horizon angle given by

$$\beta_{\max} = \arcsin\left(\frac{R}{R+H}\right)$$

and $l(\beta)$ the distance the gamma-ray travels in the Mercury surface on its way to the detector and $l_{\max}$ the maximum depth below which very few gamma-rays escape with their initial energy (roughly 2 m in our calculations). Equation (2) is solved numerically. In all the calculations, the error resulting from the applied numerical method is less than 1%.

Experiments for planetary gamma-ray spectroscopy

To study the method of planetary gamma-ray spectroscopy we simulated the process of gamma-ray production by irradiating a thick piece of matter (a Thick Target) with energetic protons provided by an accelerator. The gamma-ray flux emitted from the Thick Target was measured by a gamma-ray spectrometer consisting of a HPGe detector and a charged particle anti-coincidence shield. The resulting gamma-ray spectra were rather complex and could only be fully unravelled due to the high-resolution capability of the detector (Brückner *et al.*, 1992, 1993). The quality of the analytical method is briefly described in Fabian *et al.* (1996) and will be fully demonstrated elsewhere.

Modelling of Mercury gamma-rays

For these calculations, Mercury was modelled as a sphere with a radius of 2439 km and a surface density of 2.5 g cm^{-3}. The bulk composition of Mercury is virtually unconstrained by the present data set of Mercury. Therefore, the assumed bulk composition of Mercury is thus largely a matter of the used evolution model. The broad spectrum of models for the composition of Mercury, which are allowed by the present constraints, can range from extremely refractory-rich to extremely volatile-rich end members. To cover this wide range of compositions, we selected three bulk compositions derived from existing models presented by Goettel (1988): extreme refractory-rich, preferred, and extreme volatile-rich model (Table 2).

Table 2. Chemical composition (in wt %) of the refractory, preferred, and volatile model used in numerical simulation calculations of emitted gamma-ray fluxes (after Goettel, 1988)

Element	Refractory model	Preferred model	Volatile model
O	43.81	45.34	42.89
Na	—	0.28	1.04
Mg	20.85	22.59	19.33
Al	8.80	2.96	1.73
Si	15.23	21.51	21.05
Ca	10.88	4.02	2.17
Ti	0.43	1.01	0.08
Fe	—	2.29	11.71

Recent radar observations of Mercury have revealed the presence of anomalous radar reflectivity near the north and south poles (Slade *et al.*, 1992; Harmon and Slade, 1992; Harmon *et al.*, 1994). Thermal modelling shows that very cold maximum surface temperatures could be expected within the permanently shadowed regions of craters in the polar zones (Paige *et al.*, 1992). The apparent correlation between the location of anomalous polar radar features and the location of observed large craters in the polar regions can be attributed to the presence of water ice. At these low temperatures water ice should be stable to evaporation over large time scales. Therefore, we also investigated the possibility of water detection by calculating the gamma-ray signals for two additional compositions: 0.5 and 1% water were added to the preferred model. A homogeneous distribution of all elements in the Mercury surface was assumed in all cases. We used a temperature of 440 K for all neutron-transport calculations.

As the particle production and equilibrium spectra are strongly depth-dependent, Mercury's sphere was divided into concentric shells of varying thickness, with many layers near the surface and fewer layers at greater depths. The thickness of a shell resulted from the compromise between two opposite requirements: the minimization of statistical errors in the calculations, which are approximately inversely proportional to the shell thickness, and the investigation of the depth dependence of the particle fluxes, which can be more precisely described by splitting the investigated body into finer shells. The importance of the second requirement is underscored by the fact that in the energy range of interest about 90% of all gamma-rays reaching the surface come from depths of less than one mean thickness ($1/\mu$), where μ is the mass attenuation coefficient.

Calculated gamma-ray fluxes

In the following we present the results of gamma-ray flux calculations including counting times. We would like to

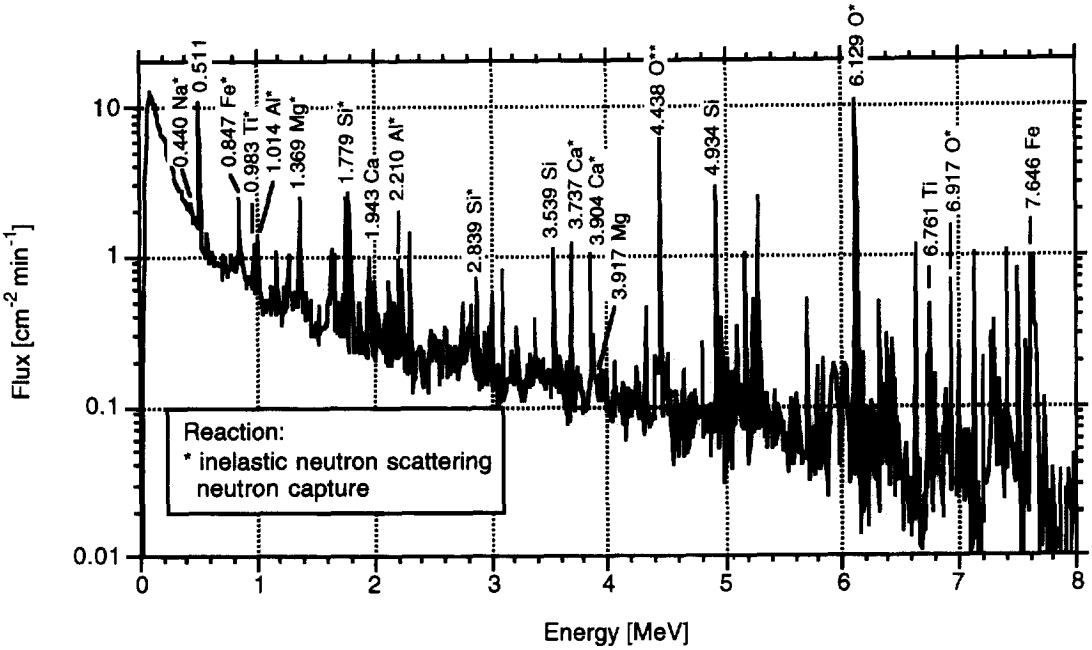

Fig. 1. Gamma-ray flux spectrum emitted by the "preferred" Mercury surface composition (cf. Table 2)

point out that these values were calculated, entirely; no scaling of measured data was applied. The following codes were used: (1) the above presented LCS package for neutron depth profiles and fluxes, general gamma-ray continuum (background), and capture gamma-ray fluxes, (2) a code for inelastic gamma-ray fluxes, (3) a code for transport of gamma-rays out of the surface towards the detector (in orbit), (4) the Monte-Carlo code ACCEPT (Halbleib and Mehlhorn, 1984) for detector efficiency, and (5) a code for counting errors and counting times.

The expected gamma-ray flux spectrum emitted by the "preferred" Mercury composition (Table 2) is presented in Fig. 1 showing the many discrete-energy gamma-ray lines and the gamma-ray continuum.

In Table 3, the gamma-ray fluxes together with counting times of the three composition models (Table 2) are listed. The counting time represents the time required to accumulate the spectrum of one pixel according to a preset error (in this case 10%). The error is derived from the peak area of the line and the underlying background for a given counting time. A characteristic gamma-ray line was selected for neutron inelastic and neutron capture reaction, each (cf. Table 3). These lines show no signs for large interferences in realistic prompt gamma-ray spectra. The lines are ordered by counting time, so showing a kind of sensitivity for each element. For the "preferred" composition, the following elements can be determined with decreasing precision: Mg, Si, O, Fe, Al, Ti, Na, and Ca. Of course, this order depends on detection sensitivity (general production reaction rate) and concentration of each element. If larger errors are allowed, the resulting counting time is accordingly shorter. Since the three com-

Table 3. Calculated gamma-ray fluxes of characteristic gamma-ray lines for three assumed Mercury compositions (cf. Table 2). "Time" is the counting time of one surface pixel to reach a required flux error of 10%. Orbit altitude is 200 km. In the refractory model, the elements Na and Fe do not exist (cf. Table 2)

	Refractory					Preferred			Volatile	
El.	Energy (MeV)	M	Flux (a)	Error 10% Time (h)	El.	Flux (a)	Error 10% Time (h)	El.	Flux (a)	Error 10% Time (h)
Mg*	1.369	I	2.406	0.2	Mg*	2.460	0.1	Mg*	2.443	0.2
Si*	1.779	I	1.562	0.3	Si*	2.270	0.1	Si*	2.324	0.2
Al*	1.014	I	0.360	1.3	O*	1.030	0.9	Fe*	1.215	0.2
O*	6.129	I	1.060	1.9	Fe*	0.210	1.0	O*	1.091	1.9
Ca	1.943	C	0.186	6.1	Al*	0.100	2.8	Na*	0.143	3.6
Si	4.934	C	0.217	7.0	Ti*	0.110	5.7	Si	0.192	8.4
Al	3.779	C	0.260	7.4	Si	0.200	7.7	Fe	0.372	10.9
Ca*	3.737	I	0.180	13.8	Na*	0.050	16.2	Al*	0.074	18.0
Mg	3.917	C	0.080	41.4	Ca*	0.080	23.6	Mg	0.069	101
Ti	6.761	C	0.100	64.5	Ti	0.120	30.9	Ca*	0.039	206
Ti*	0.983	I	0.034	82.1	Ca	0.040	73.0	Ca	0.024	232
Na*	0.440	I	—		Mg	0.080	75.1	Al	0.033	273
Fe*	0.847	I	—		Al	0.050	95.3	Ti*	0.007	1597
Fe	7.646	C	—		Fe	0.070	118	Ti	0.010	3359

M = Mode; I = inelastic neutron scattering reaction (also asterisk *); C = neutron capture reaction; a = photons cm^{-2} min^{-1}.

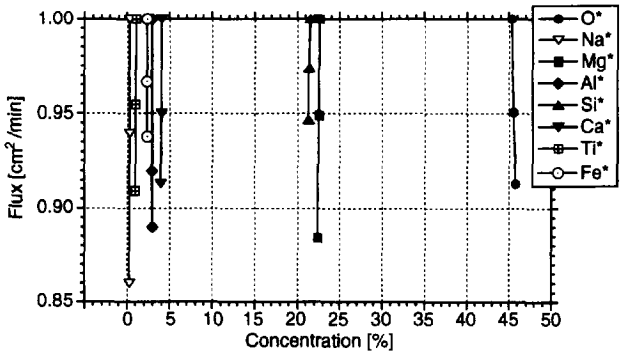

Fig. 2. Inelastic gamma-ray fluxes (normalized to dry case) at 200 km altitude above Mercury for the compositions: "preferred" (cf. Table 2), preferred containing 0.5 and 1% water

positions produce unique gamma-ray signal patterns, the three models can be distinguished, clearly. In the case of a Mercury mission, one receives gamma-ray spectra emitted by surface areas of unknown composition. The measured gamma-ray flux will be compared with the calculated fluxes of the three basic compositions. In an iterative process, a chemical composition will be derived that fits the measured gamma-ray fluxes the best.

To investigate the sensitivity of detecting water in the polar regions, we calculated the gamma-ray fluxes for three assumed compositional cases: the preferred composition (cf. Table 2) with no water, 0.5 and 1% water content. In order to visualize changes of the gamma-ray signals for different lines, we normalized the gamma-ray fluxes of the "wet" cases to the flux of the dry "preferred" composition.

In Fig. 2, inelastic gamma-ray lines of the elements O, Na, Mg, Al, Si, Ca, Ti, and Fe can be seen for the three cases. It should be noted that the admixture of water decreases the concentration of the other elements somewhat, since the sum of all elements is always normalized to 100%. As expected, the inelastic gamma-ray fluxes, which result from the interaction of fast neutrons (energies above 100 keV), decrease with increasing water content, i.e. with increasing moderation of neutrons.

In Fig. 3, capture gamma-ray lines of Mg, Al, Si, Ca, Ti, and Fe are shown for the three cases, as described above. Here, drastic effects can be seen for the two wet compositions, since the energy and number of the thermal neutrons is strongly affected by moderating material. More neutrons reach thermal energies and undergo a capture reaction before they escape the surface. Compared to the dry case, an average increase of 20–30% for the admixture of 0.5% water, and an increase of 40–55% for the 1% water case is observed.

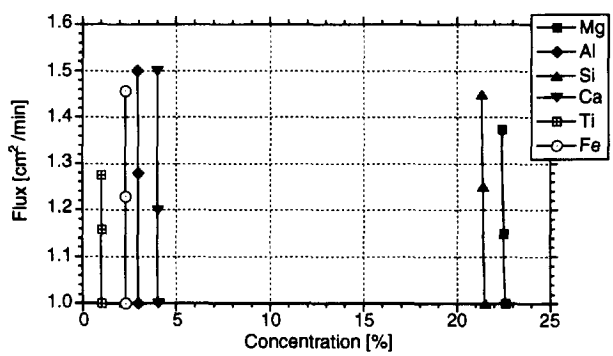

Fig. 3. Capture gamma-ray fluxes (normalized to dry case) at 200 km altitude above Mercury for the compositions: "preferred" (cf. Table 2), preferred containing 0.5 and 1% water

This demonstrates clearly that possible small amounts of water in the polar regions can easily be detected by a gamma-ray spectrometer: besides the direct signal of hydrogen (not shown in the figures), all major elements will reveal the presence of water by increased or decreased gamma-ray fluxes. To make the simulation simple, a homogeneous distribution of water in the Mercury surface was assumed in all cases. We are aware, that a patchy distribution of permanently shaded ice needs a more detailed modelling, however, our model can be considered as the equivalent to thick patchy ice plates mixed with normal surface soil and evenly spread over one spatial pixel.

Orbital gamma-ray spectrometer

The Mercury Orbiter studied by ESA (Grard *et al.*, 1994) had four instruments as primary scientific payload: magnetometer, imaging camera, gamma-ray spectrometer, and plasma ion sensor. The spacecraft that has to withstand the strenuous thermal environment (up to 25 $W m^{-2}$) of the Mercury orbit, used a spin-stabilized design. The orbit that had to fulfil requests from all instruments was polar elliptical with a periherm of 200–300 km and an apherm of 15,000–20,000 km. Such an orbit would ensure good surface coverage (1) at low altitude for remote sensing and (2) at high altitude for magnetospheric/plasma measurements. The nominal mission was at last three Mercury years (263 terrestrial days).

The gamma-ray measurements have to take into account the omni-directional response of the spectrometer and a varying field of view. Since the gamma-ray production in the surface is depth dependent, collimation of the gamma-rays restricts the effective field of view as a function of the altitude of the spacecraft and this is included in our approach to calculate gamma-ray fluxes. A footprint (or pixel) can be defined as an area on the planet, where 80% of the radiation originates. Assuming a polar orbit during a nominal mission, the planetary regions will be covered according to their latitude. The spacecraft will fly over the pole during each orbit, while it will pass the same footprint on the equator only a few times during the mission. The gamma-ray spectrometer will make short measurements (20–60 s) over each footprint to obtain sufficient spatial resolution. On Earth, the individual spectra will be stored in a data base to permit summing of the spectra according to selection criteria, such as time or position on the surface. In the beginning of the mission, one can sum spectra of only large regions to get good statistics; later on, smaller and smaller regions will be spatially resolved and the planet can be subdivided according to geological units and morphological criteria. Finally, maps from Mercury can be overlaid with concentration variations of each element detected. Of course, the spatial resolution of the gamma-ray data will be coarse, but, these concentration maps will provide invaluable information about the surface of Mercury. From

the surface composition the mantle composition can be derived providing constraints for the various evolution models of Mercury.

Detector

To achieve detailed measurements of the Mercurian gamma-rays, a high-purity germanium (HPGe) detector is considered to be the best choice. The advantage of a HPGe detector system is based on its excellent energy-resolution, which facilitates the evaluation of the measured gamma-ray spectra, tremendously. There are also some inconveniences, such as: (1) the Ge crystal has to be cooled down to temperatures below 120 K; (2) the Ge crystal is subject to radiation damage induced by cosmic-ray particles or by strong solar flares. If the Ge crystal can be kept below 90 K, one year of good performance can be achieved, provided no strong solar flares occur, otherwise, the energy resolution can degrade so much that removal of the damage is necessary. This can be done by heating the crystal up to temperatures of 100°C for several tens of hours to obtain the original energy resolution, again. More details about detector radiation damage can be found in Brückner *et al.* (1991) and Koenen *et al.* (1995).

Cooling of the Ge crystal in the hot Mercury orbit will preferentially be done by using an active cooling device, such as a Stirling cooler. It seems that current coolers are not yet mature for such a mission (they are either too heavy or need too much power, besides vibrational problems that deteriorate the performance of the detector); but, given several years of further development, a space-proof lightweight Stirling cooler seems to be achievable. Therefore, the option for a HPGe gamma-ray spectrometer on board a Mercury orbiter can be kept open. In case a suitable cooler will not be available, a scintillation detector, such as NaI or CsI, could be used. Because of their poorer energy resolution compared to HPGe detectors, restrictions on the evaluation of the Mercurian spectra have to be taken into account. However, basic information will be obtained by any detector type. The NEAR XGRS project will demonstrate the feasibility of scintillation technology (Trombka *et al.*, 1995). However, for a very ambitious mission, such as a Mercury orbiter, a germanium gamma-ray spectrometer is the first choice.

Conclusion

For a future Mercury orbiter mission, a gamma-ray spectrometer will be an invaluable instrument to provide data on the elemental composition of the surface. Model calculations assuming three different surface compositions and different water concentrations were performed using elaborate Monte-Carlo codes. The results clearly show: (1) the gamma-ray data allow to characterize different types of surfaces, (2) small concentrations of potential water buried in the polar regions can easily be detected. In addition, elemental composition of regions on the surface will be determined. These data can further be used to derive constraints for models on origin and evolution of Mercury. A germanium detector seems to be the favourite detector for such a task because of its superior energy resolution.

Acknowledgements. We would like to thank U. Fabian, M. Koenen, and G. Dreibus for assistance. We acknowledge the generous support of H. Wänke.

References

Anderson, J. D., Colombo, G., Esposito, P. B., Lau, L. E. and Trager, G. B. (1987) The mass, gravity field, and ephemeris of Mercury. *Icarus* **71**, 337–349.

Armstrong, T. W. (1972) Calculation of the lunar photon albedo from galactic and solar proton bombardment. *J. Geophys. Res.* **77**, 524–536.

Arnold, J. R. (1958) The gamma spectrum of the Moon's surface. *Proc. Lunar Planet. Explorat. Coll.* 1(3), pp. 28–31. Space Inf. Syst. Div., North American Aviation, Inc., Downey, California.

Arnold, J. R., Metzger, A. E., Anderson, E. C. and Van Dilla, M. A. (1962) Gamma rays in space, Ranger 3. *J. Geophys. Res.* **67**, 4878–4880.

Arnold, J. R., Boynton, W. V., Englert, P., Feldman, W. C., Metzger, A. E., Reedy, R. C., Squyres, S. W., Trombka, J. I. and Wänke, H. (1989) Scientific considerations in the design of the Mars Observer Gamma-Ray Spectrometer. In *High-Energy Radiation Background in Space*, eds Rester and Trombka, AIP Conf. Proc. 186, pp. 453–466. Am. Inst. Phys., New York.

Asker, J. R. (1995) Moon mission set for 1997. Aviation Week and Space Technology, March 6, pp. 18–20.

Bielefeld, M. J., Reedy, R. C., Metzger, A. E., Trombka, J. I. and Arnold, J. A. (1976) Surface chemistry of selected lunar regions. *Proc. Lunar Sci. Conf. 7th. Geochim. Cosmochim. Acta Suppl.* **7**, 2662–2676.

Boynton, W. V., Trombka, J. I., Feldman, W. C., Arnold, J. R., Englert, P. A. J., Metzger, A. E., Reedy, R. C., Squyres, S. W., Wänke, H., Bailey, S. H., Brückner, J., Callas, J. L., Drake, D. M., Duke, P., Evans, L. G., Haines, E. L., McCloskey, F. C., Mills, H., Shinohara, C. and Starr, R. (1992) Science applications of the Mars Observer Gamma Ray Spectrometer. *J. Geophys. Res.* **97**(E5), 7681–7698.

Briesmeister, J. F. (1993) MCNP—a general Monte Carlo N-particle transport code, version 4A. Los Alamos National Laboratory report LA-12625-M, p. 693.

Brückner, J., Wänke, H. and Reedy, R. C. (1987) Neutron-induced gamma ray spectroscopy: simulations for chemical mapping of planetary surfaces. *Proc. 17th Lunar Planet. Sci. Conf.*, Part 2. *J. Geophys. Res.* **92**(B4), E603–E616.

Brückner, J., Körfer, M., Wänke, H., Schroeder, A. N. F., Filges, D., Dragovitsch, P., Englert, P. A. J., Starr, R., Trombka, J. I., Taylor, I., Drake, D. M. and Shunk, E. R. (1991) Proton-induced radiation damage in germanium detectors. *IEEE Trans. Nucl. Sci.* **38**(2), 209–217.

Brückner, J., Fabian, U., Patnaik, A., Wänke, H., Cloth, P., Dagge, G., Drüke, V., Filges, D., Englert, P. A. J., Drake, D. M., Reedy, R. C. and Parlier, B. (1992) Simulation experiments for Planetary Gamma-Ray Spectroscopy by means of thick target high-energy proton irradiations. *Lunar Planet. Sci.*, Vol. XXIII, pp. 169–170. Lunar Planet. Inst., Houston.

Brückner, J., Fabian, U., Wänke, H., Drüke, V., Filges, D. and Neef, R. D. (1993) Simulation of planetary gamma ray spectroscopy by thick target irradiation experiments. *Proc. 8th Int. Symp. Capture Gamma-Ray Spectroscopy Related Topics*, Fribourg, Switzerland, Sept. 20–24, pp. 980–982. World Scientific, London.

Brückner, J., Fabian, U. and Wieder, M. (1994) Considerations

for planetary gamma-ray spectroscopy of the surface of Mercury. *Lunar Planet. Sci.*, Vol. XXV, pp. 187–188. Lunar Planet. Inst., Houston.

Burghele, A., Dreibus, G., Palme, H., Rammensee, W., Spettel, B., Weckwerth, G. and Wänke, H. (1983) Chemistry of shergottites and the Shergotty parent body (SPB): further evidence for the two component model of planet formation. *Lunar Planet. Sci.*, Vol. XIV, pp. 80–81. Lunar Planet. Inst., Houston.

Cameron, A. G. (1985) The partial volatilization of Mercury. *Icarus* **64,** 285–294.

Cameron, A. G. W., Fegley Jr, B., Benz, W. and Slattery, W. L. (1988) The strange density of Mercury: theoretical considerations. In *Mercury*, eds Vilas *et al.*, pp. 692–708. Arizona University Press, Tucson.

Castagnoli, G. C. and Lal, D. (1980) Solar modulation effects in terrestrial production of carbon-14. *Radiocarbon* **22,** 133–158.

Chicarro, A., Racca, G. and Coradini, M. (1994) MORO—a European Moon-orbiting observatory for global Lunar characterization. *ESA J.* **18,** 183–195.

Dagge, G., Dragovitsch, P., Filges, D. and Brückner, J. (1991) Monte Carlo simulation of martian gamma-ray spectra induced by galactic cosmic rays. *Proc. Lunar Planet. Sci. Conf.*, Vol. 21, pp. 425–435.

Davis, P. A. and Spudis, P. D. (1985) Petrologic province maps of the Lunar Highlands derived from orbital geochemical data. *Proc. Lunar Planet. Sci. Conf.* 16*th*. *J. Geophys. Res.* **90,** D61–D74.

Davis, P. A. and Spudis, P. D. (1987) Global petrologic variations on the Moon: a ternary-diagram approach. *Proc. Lunar Planet. Sci. Conf.* 17*th*. *J. Geophys. Res.* **92,** E387–E395.

d'Uston, C., Borrel, V., Boynton, W. V., Brückner, J., Klinger, J., Reedy, R. C., Schmitt, B. and Trombka, J. I. (1996) Gamma-ray spectroscopy for the investigation of the comet chemical composition on board Champollion. *Lunar Planet. Sci.*, Vol. XXVII, pp. 327–328. Lunar Planet. Inst., Houston.

Englert, P. A. J., Chakravarty, N., Ivanova, O., Beck, E. A., Brückner, J., Bailey, S. H., McCloskey, F. C. and Boynton, W. V. (1994) Gamma ray spectra from the Mars Observer Gamma Ray Spectrometer: cruise data analysis. *Lunar Planet. Sci.*, Vol. XXV, pp. 353–354. Lunar Planet. Inst., Houston.

Fabian, U., Masarik, J., Brückner, J., Koenen, M., Wänke, H., Englert, P. A. J., Drake, D. M., Drüke, V., Neef, R. D. and Filges, D. (1996) Thick target experiments and Monte Carlo calculations for planetary gamma ray spectroscopy. *Lunar Planet. Sci.*, Vol. XXVII, pp. 347–348. Lunar Planet. Inst., Houston.

Goettel, K. A. (1988) Present bounds on the bulk composition of Mercury: implications for planetary formation processes. In *Mercury*, eds Vilas *et al.*, pp. 613–621. Arizona University Press, Tucson.

Grard, R., Scoon, G. and Coradini, M. (1994) Mercury Orbiter—an interdisciplinary mission. *ESA J.* **18,** 197–205.

Halbleib, J. A. and Mehlhorn, T. A. (1984) ITS: the integrated TIGER series of coupled electron/photon Monte Carlo transport codes, Sandiat Nat. Lab. preprint SAND 84-0573, pp. 1–99.

Harmon, J. K. and Slade, M. A. (1992) Radar mapping of Mercury: full-disk images and polar anomalies. *Science* **258,** 640–643.

Harmon, J. K., Slade, M. A., Vélez, R. A., Crespo, A., Dryer, M. J. and Johnson, J. M. (1994) Radar mapping of Mercury's polar anomalies. *Nature* **369,** 213–215.

Harrington, T. M., Marshall, J. H., Arnold, J. R., Peterson, L. E., Trombka, J. I. and Metzger, A. E. (1974) The Apollo gamma-ray spectrometer. *Nucl. Inst. Meth.* **118,** 401–411.

Koenen, M., Brückner, J., Körfer, M., Taylor, I. and Wänke, H. (1995) Radiation damage in large-volume n- and p-type high-purity germanium detectors irradiated by 1.5 GeV protons. *IEEE Trans. Nucl. Sci.* **42,** 653–658.

Masarik, J. and Reedy, R. C. (1994a) Effects of bulk chemical composition on nuclide production processes in meteorites. *Geochim. Cosmochim. Acta* **58,** 5307–5317.

Masarik, J. and Reedy, R. C. (1994b) Numerical simulation of planetary gamma-ray spectra induced by galactic cosmic rays. In *Proc. Int. Conf. Nucl. Data for Sci. Techn.*, ed. J. K. Dickens, pp. 551–553. Am. Nucl. Soc., La Grange Park, Illinois.

Masarik, J. and Reedy, R. C. (1996) Gamma ray production and transport in Mars. *J. Geophys. Res.* **E101,** 18,891–18,912.

Metzger, A. E., Van Dilla, M. A., Anderson, E. C. and Arnold, J. R. (1962) Ranger gamma ray spectrometer. *Nucleonics* **20**(10), 64–66.

Metzger, A. E., Anderson, E. C., Van Dilla, M. A. and Arnold, J. R. (1964) Detection of interstella flux of gamma rays. *Nature* **204,** 766–767.

Metzger, A. E., Trombka, J. I., Peterson, L. E., Reedy, R. C. and Arnold, J. R. (1972) A first look at the Lunar orbital gamma ray data. *Proc. Lunar Sci. Conf.* 3*rd*, Vol. 3, Frontispiece.

Metzger, A. E., Haines, E. L., Parker, R. E. and Radocinski, R. G. (1977) Thorium concentrations in the lunar surface. I: Regional values and crustal content. *Proc. Lunar Sci. Conf.* 8*th*, pp. 949–999.

Michlovich, E. S., Vogt, S., Masarik, J., Reedy, R. C., Elmore, D. and Lipschutz, M. E. (1994) ^{26}Al, ^{10}Be, and ^{36}Cl depth profiles in the Canyon Diablo meteorite. *J. Geophys. Res.* **99,** 22187–22194.

Mitrofanov, I. G., Anfimov, D. S., Chernenko, A. M., Dolidze, V. Sh., Pozanenko, A. S., Ushakov, D. A., Auchampaugh, G. F., Cafferty, M., Drake, D. M., Fenimore, E. E., Klebesadel, R. W., Longmire, J. L., Moss, C. E., Reedy, R. C. and Valencia, J. E. (1995) A high precision gamma-ray spectrometer for the Mars-94 Mission. *Acta Astron.* **35**(Suppl.), 119–126.

Paige, D. A., Wood, S. E. and Vasavada, A. R. (1992) The thermal stability of water ice at the poles of Mercury. *Science* **258,** 643–646.

Plechaty, E. E., Cullen, D. E. and Howerton, R. J. (1981) Tables and graphs of photon-interaction cross sections from 0.1-keV to 100-MeV derived from the LLL evaluated nuclear-data library. Lawrence Livermore Laboratory Rep. UCRL-50400, Vol. 6, Rev. 3.

Prael, R. E. and Lichtenstein, H. (1989) User guide to LCS. The LAHET Code System. Los Alamos Nat. Lab. Rep., LA-UR-89-3014, 76 pp.

Reedy, R. C. (1978) Planetary gamma-ray spectroscopy. *Proc. Lunar Planet. Sci. Conf.* 9*th*. *Geochim. Cosmochim. Acta Suppl.* **10,** 2961–2984.

Reedy, R. C. (1979) Elemental analysis of planetary surfaces via orbital gamma ray spectroscopy. In *Computers Activation Analysis Gamma-Ray Spectroscopy*, eds B. S. Carpenter *et al.*, US DOE CONF-780421, pp. 684–697.

Reedy, R. C. (1987) Nuclide production by primary cosmic-ray protons. *J. Geophys. Res.* **92,** E697–E702.

Reedy, R. C., Arnold, J. R. and Trombka, J. I. (1973) Expected gamma ray spectra from the lunar surface as a function of chemical composition. *J. Geophys. Res.* **78,** 5847–5866.

Shea, M. A., Smart, D. F., Adams Jr, J. H., Chenette, D., Feynman, J., Hamilton, D. C., Heckman, G., Konradi, A., Lee, M. A., Nachtwey, D. S. and Roelof, E. C. (1988) Toward a descriptive model of solar particles in the heliosphere. In *Interplanet. Particle Environ.*, eds J. Feynman and S. Gabriel, JPL Pub. 88-28, pp. 3–13. Jet Propul. Lab., Pasadena, California.

Simpson, J. A. (1983) Elemental and isotopic composition of the galactic cosmic rays. *Annu. Rev. Nucl. Part. Sci.* **33,** 323–381.

Slade, M. A., Butler, B. J. and Muhleman, D. O. (1992) Mercury radar imaging: evidence for polar ice. *Science* **258,** 635–640.

Spudis, P. D. and Hawke, B. R. (1981) Chemical mixing model studies of Lunar orbital geochemical data: Apollo 16 and 17 highland compositions. *Proc. Lunar Planet. Sci. Conf.* 12*b*, pp. 781–789.

Surkov, Yu. A. (1984) Nuclear-physical methods of analysis in Lunar and planetary investigations. *Isotopenpraxis* **20,** 321–329.

Surkov, Yu. A., Barsukov, V. L., Moskaleva, L. P., Kharyukova, V. P., Zaitseva, S. Ye., Smirnov, G. G. and Manvelyan, O. S. (1989) Determination of the elemental composition of martian rocks from Phobos 2. *Nature* **341,** 595–598.

Surkov, Yu. S. *et al.* (1975) *Kosmich. Issled.* (*Cosmic Res.*) XIV.

Thakur, A. N. and Arnold, J. R. (1993) A sensitive continuum analysis method for gamma ray spectra. *Nucl. Instrum. Meth. Phys. Res.* **A325,** 529–536.

Trombka, J. I., Evans, L. G., Starr, R., Floyd, S. R., Squyres, S. W., Whelan, J. T., Bamford, G. J., Coldwell, R. L., Rester, A. C., Surkov, Yu. A., Moskaleva, L. P., Kharyukova, V. P., Manvelyan, O. S., Zaitseva, S. Ye. and Smirnov, G. G. (1992) Analysis of the Phobos mission gamma-ray spectra from Mars. *Proc. Lunar Planet. Sci.*, Vol. 22, pp. 23–29. Lunar Planet. Inst., Houston.

Trombka, J. I., Boynton, W. V., Brückner, J., Squyres, S. W., Bailey, S. H., Clark, P. E., Evans, L. G., Floyd, S. R., Starr, R., Gold, R., Goldstein, J. and McNutt, R. (1995) The X-ray/gamma-ray spectrometer for the NEAR mission. *Lunar Planet. Sci.*, Vol. XXVI, pp. 1421–1422. Lunar Planet. Inst., Houston.

Vinogradov, A. P., Surkov, Yu. A., Chernov, G. M., Kirnozov, F. F. and Nazarkina, G. B. (1967) Lunar gamma radiation and the composition of the Lunar rocks according to the results of a Luna-10 experiment. *Cosmic Res.* **5,** 741–753, transl. *Kosmicheskie Issledovaniya* **5,** 874–890.

Wänke, H. (1987) Chemistry and accretion of Earth and Mars. *Bull. Soc. Géol. Fr.* **1987**(8), 13–19.

Wänke, H. and Dreibus, G. (1986a) Mercury, a highly reduced planet? Mercury Conf., Tucson, Arizona, August 6–9, Abstract.

Wänke, H. and Dreibus, G. (1986b) Die chemische Zusammensetzung und Bildung der terrestrischen Planeten. *Mitteilungen Astronom. Gesell.* **65,** 9–24.

Wetherill, G. W. (1988) Accumulation of Mercury from Planetesimals. In *Mercury*, eds Vilas *et al.*, pp. 670–691. Arizona University Press, Tucson.